

## Spatial Distribution of Marine Crenarchaeota Group I in the Vicinity of Deep-Sea Hydrothermal Systems

Ken Takai,<sup>1\*</sup> Hanako Oida,<sup>1</sup> Yohey Suzuki,<sup>1</sup> Hisako Hirayama,<sup>1</sup> Satoshi Nakagawa,<sup>2</sup>  
Takuro Nunoura,<sup>1</sup> Fumio Inagaki,<sup>1</sup> Kenneth H. Nealson,<sup>1,3</sup>  
and Koki Horikoshi<sup>1</sup>

*Subground Animalcule Retrieval Project, Frontier Research System for Extremophiles, Japan Marine Science & Technology Center, Yokosuka 237-0061,<sup>1</sup> and Laboratory of Molecular Marine Microbiology, Division of Applied Biological Science, Graduate School of Agriculture, Kyoto University, Kitashirakawa, Kyoto 606-8502,<sup>2</sup> Japan, and Department of Earth Sciences, University of Southern California, Los Angeles, California 90089-0740<sup>3</sup>*

Received 20 August 2003/Accepted 12 December 2003

**Distribution profiles of marine crenarchaeota group I in the vicinity of deep-sea hydrothermal systems were mapped with culture-independent molecular techniques. Planktonic samples were obtained from the waters surrounding two geographically and geologically distinct hydrothermal systems, and the abundance of marine crenarchaeota group I was examined by 16S ribosomal DNA clone analysis, quantitative PCR, and whole-cell fluorescence in situ hybridization. A much higher proportion of marine crenarchaeota group I within the microbial community was detected in deep-sea hydrothermal environments than in normal deep and surface seawaters. The highest proportion was always obtained from the ambient seawater adjacent to hydrothermal emissions and chimneys but not from the hydrothermal plumes. These profiles were markedly different from the profiles of epsilon-Proteobacteria, which are abundant in the low temperatures of deep-sea hydrothermal environments.**

The members of marine crenarchaeota group I (MGI) are the most abundant and widely distributed *Archaea* in the global ocean biosphere from surface to bottom waters and from polar to tropical regions (6–8, 11, 12, 20, 19, 28, 29, 31, 36, 46, 48, 52, 54–56). Since the first discovery of the occurrence of MGI in coastal waters (6, 11), culture-independent molecular surveys have expanded the potential habitats for MGI from marine planktonic fractions to seafloor surfaces (20, 55, 56), deep subseafloor sediments (16, 17), marine hydrothermal systems (31, 46, 48), freshwater lakes (26, 39), and deep terrestrial subsurface aquifers (52). Despite their ubiquity in the global aquatic biosphere and the diversity of genes and genomic structures based on rRNA genes (rDNA) and genome fragments obtained directly from environments (3, 4, 40, 44), their physiological features and ecological significance are still unclear due to the lack of success in cultivating them.

Recent investigations have begun to provide insights into the metabolic modes and trophic types represented by the MGI. Ouverney and Fuhrman (33), with a technique called substrate tracking autoradiography fluorescence in situ hybridization, demonstrated that members of the MGI were capable of assimilating dissolved amino acids. In contrast, stable carbon isotopic analyses of archaeal membrane lipids (glycerol dibiphytanyl glycerol tetraethers) in the water columns and sediments suggested that most MGI members might be autotrophs, with bicarbonate as a primary carbon source (15, 21, 22, 41, 42). Analysis of the archaeal lipids recovered from

sediments based on radiocarbon isotopes also supported the nonphototrophic bicarbonate-dependent carbon metabolism of the MGI members (35). Further evidence for autotrophy in MGI was clearly demonstrated by in situ [<sup>13</sup>C]bicarbonate tracer experiments (58).

In the absence of cultivated organisms, it has been difficult to discern much about the energy metabolism of the MGI members. One might hope that scrutiny of the distribution and abundance of MGI in various environments would provide insights into their physiology. To this end, studies of the distribution of *Archaea* closely related to the MGI by DeLong et al. (7) and Karner et al. (19) suggested that this group might be aerobic psychrophiles widely occurring in the subphotic zone of the ocean. In contrast, analysis of archaeal membrane lipids in the euxinic zone of the Arabian Sea (43) suggested that the MGI may be interface microorganisms, living at an oxic-anoxic boundary in the water column as nitrate-reducing chemolithoautotrophs (43). Other studies by Moyer et al. (31) suggest that deep-sea hydrothermal systems are potential sources and sinks of marine planktonic *Archaea* (31) and that the MGI might be the dominant archaeal components in hydrothermal sediments and chimneys (46, 48, 51). Nevertheless, the quantities and distribution profiles of MGI members in deep-sea hydrothermal environments have not been yet determined. In this study, the spatial distribution of MGI in the vicinity of deep-sea hydrothermal systems was characterized by culture-independent molecular techniques.

### MATERIALS AND METHODS

**Sample sites, collection, and processing.** Hydrothermal plume and seawater samples were obtained from two geographically and geologically distinct deep-sea hydrothermal systems: the Kairei Field in the Central Indian Ridge (49) of the Indian Ocean, and Iheya North in the Okinawa Trough off Japan (49, 50).

\* Corresponding author. Mailing address: Subground Animalcule Retrieval Project, Frontier Research System for Extremophiles, Japan Marine Science & Technology Center, 2-15 Natsushima-cho, Yokosuka 237-0061, Japan. Phone: 81-468-67-9677. Fax: 81-468-67-9715. E-mail: kent@jamstec.go.jp.

Both sites were sampled with manned submersibles, the Kairei Field with the *Shinkai 6500* (YK01-15 cruise conducted in January to March 2002), and the Iheya North with the *Shinkai 2000* (YK02-06 cruise conducted in April to May 2002). In the Kairei Field, the Kali chimney (25°19.2194'S, 70°02.3850'E; water depth, 2,451 m) and the Fugen chimney (25°19.2165'S, 70°02.4445'E; water depth, 2,422 m) were located in the west-east direction separated by about 50 m (Fig. 1A).

In Iheya North, two chimney mounds named North Big Chimney (NBC) (27°47.451'N, 126°53.799'E; water depth, 968 m) and South Big Chimney (27°47.413'N, 126°53.800'E; water depth, 978 m) were the focus of our studies. In this hydrothermal field, vigorous hydrothermal vents including North Big Chimney and South Big Chimney were located in the north-south direction, probably along a subsurface fault, with North Big Chimney being a hydrothermal activity center (Fig. 2A). The temperature of the water was measured with a conductivity-temperature-depth profiler and a self-recording temperature probe carried by the submersible. The area around the study site was characterized with a conductivity-temperature-depth-turbidity profiler, an in situ geochemical anomaly monitoring system (13), and an altitude meter. The data obtained from these systems were used to construct the sampling maps around the study sites as shown in Fig. 1 and 2. The reference surface seawater samples were designated Indian surface and Iheya surface for the Kairei Field and Iheya North, respectively. The normal deep-seawater samples designated Indian-2380m, Iheya-500m and Iheya-900m were obtained at water depths of 2,380, 500, and 900 m, respectively, above the deep-sea hydrothermal fields. KASW-5m was ambient seawater obtained 5 m from the Kali chimney, and FASW-5m and FASW-10m were from points 5 and 10 m distant, respectively, from the Fugen chimney. In a similar manner, NBCASW-2m, NBCASW-10m, NBCASW-25m, and NBCASW-32m were ambient seawater samples obtained 2, 10, 25, and 32 m, respectively, from the North Big Chimney, and SBCASW-5m was obtained 5 m from the South Big Chimney. KP-Xm, FP-Xm, and NBCP-Xm are plume water samples obtained X meters from a vent orifice of Kali Chimney, Fugen Chimney, and North Big Chimney, respectively.

**Sample processing and total cell counts.** At both study sites, on the bases of the chimneys, ambient seawater associated with hydrothermal activity, and normal deep-sea water were sampled with both multiple Niskin water samplers and a water pumping system (37) (maximum, 20 liters) (Fig. 1 and 2).

Approximately 30 ml of each water sample was inactivated by adding formalin (final concentration, 3.7%) and preserved at 4°C. The remainder of each sample was immediately filtered onboard with cellulose acetate filters (0.22- $\mu$ m pore size). Half of the filter was preserved in 3 ml of filter-sterilized seawater containing 3.7% (vol/vol) formalin, and the other half was frozen at -80°C prior to experiments.

With formalin-fixed water samples, microbial population density was determined by 4',6-diamidino-2-phenylindole (DAPI) staining for direct counts as described previously (46, 51). Briefly, 10 ml of the formalin-fixed samples was filtered with 0.22- $\mu$ m-pore-size, 13-mm-diameter polycarbonate filters (Advantec). Each filter was rinsed twice with 10 ml of MJ synthetic seawater (38), which had been filtered through a 0.22- $\mu$ m-pore-size filter and autoclaved, and then stained by treatment with MJ seawater containing DAPI (10  $\mu$ g/ml) at 4°C overnight. The filter was rinsed twice with 10 ml of MJ seawater and examined under epifluorescence with an Olympus BX51 epifluorescence microscopy with the SPOT RT Slider charge-coupled device camera system (Diagnostic Instruments Inc.). Three filters from each sample were prepared, and the microbial cells in at least  $5 \times 10^{-7}$  m<sup>2</sup> on each filter were counted. An average of the total cell counts from the three filters was determined.

**Phylogenetic characterization and quantification of MGI rDNA.** The archaeal ribosomal DNA (rDNA) community structure and the proportion of archaeal rDNA in the whole microbial DNA assemblage obtained from water samples at the Kairei Field were determined. Microbial DNA was directly extracted from a filter frozen at -80°C with a soil DNA megaprep kit (Mo Bio Laboratories, Inc., Solana Beach, Calif.), following the manufacturer's suggested protocol. A blank tube (with no sample added) was processed as a negative control (53). Quantification of the archaeal rDNA in the whole microbial DNA assemblage was performed by a quantitative fluorescent PCR method with TaqMan probes as previously described (47). A dilution series of each of the DNA samples was prepared, and the samples were assayed with the universal rDNA mixture and the archaeal rDNA mixture (47) as the standards for quantification of whole microbial rDNA and archaeal rDNA, respectively. This analysis provided the quantities of archaeal rDNA and whole microbial rDNA, and the proportion of archaeal rDNA within the whole microbial rDNA was calculated (47).

Archaeal rDNA was amplified by PCR with LA *Taq* polymerase (TaKaRa, Kyoto, Japan). The oligonucleotide primers used were Arch21F and Arch958R (6). Reaction mixtures were prepared in which the concentration of each oligo-

nucleotide primer was 0.4  $\mu$ M and that of the DNA template was 0.1 ng  $\mu$ l<sup>-1</sup>. Thermal cycling was performed with a GeneAmp 9700 (Perkin-Elmer, Foster City, Calif.), and the conditions were as follows: denaturation at 96°C for 20 s, annealing at 50°C for 45 s, and extension at 72°C for 120 s for a total of 30 cycles. When no apparent product was recovered after 30 cycles of reaction, the number of cycles was extended to 45. The purified rDNA was cloned in vector pCR2.1 with the Original TA cloning kit (Invitrogen, Carlsbad, Calif.). The inserts were amplified by direct PCR from a single colony with M13 primers (23), treated with exonuclease I and shrimp alkaline phosphatase (Amersham Pharmacia Biotech, Buckinghamshire, United Kingdom), and directly sequenced by the dideoxynucleotide chain termination method with a dRhodamine sequencing kit (PE Applied Biosystems) following the manufacturer's recommendations.

The Arch21F primer was used in partial sequencing analysis. Single-stranded sequences approximately 400 nucleotides in length were analyzed. Sequence similarity among the single-stranded sequences was analyzed with the FASTA program supplied with the DNASIS software (Hitachi Software, Tokyo, Japan). rDNA sequences having  $\geq 97\%$  similarity as determined by the FASTA program were assigned to the same clone type. Sequences of representative rDNA clones approximately 0.95 kb in length were determined from both strands. The sequences were manually aligned to prokaryotic small-subunit rDNA data from Ribosomal Data Project II (RDP-II) (27) and other databases based on primary and secondary structure considerations. Phylogenetic analyses were restricted to nucleotide positions between the Arch21F and Arch958R primers that were unambiguously alignable in all sequences. Neighbor-joining analysis was performed with the PHYLIP package (version 3.5; obtained from J. Felsenstein, University of Washington, Seattle). Bootstrap analysis was used to provide confidence estimates for phylogenetic tree topologies.

**Whole-cell FISH analysis.** In order to examine the specific distribution of MGI on the cell level in the vicinity of deep-sea hydrothermal systems, whole-cell fluorescence in situ hybridization (FISH) analysis targeting 16S rRNA was conducted. The target microbial populations were whole microbial cells (DAPI-stained cell fraction and universal probe-binding cell fraction), MGI cells (MGI-specific probe-binding cell fraction), and the epsilon subdivision of the *Proteobacteria* (epsilon-*Proteobacteria*-specific probe-binding fraction).

An rRNA-targeted oligonucleotide probe (MGI 391) specifically binding to MGI rRNA was previously designed for detection of a diversity of MGI members (46). In this study, a slightly modified probe was prepared with an almost identical binding site but with 2 bases added at its 5' end to elevate its melting temperature, designated the MGI 391-413 probe (5'-GGAAAYCACTCGGAYTAACCTT-3'; Y = C or T), which corresponded to positions 319 to 413 in *Escherichia coli* 16S rDNA. In order to find an rRNA-targeted oligonucleotide probe specifically but commonly binding to an increasing number of epsilon-proteobacterial rRNAs, a multiple alignment of various rDNA sequences representing epsilon-proteobacterial subgroups, including newly isolated deep-sea hydrothermal thermophilic and mesophilic strains (49), was constructed.

Among several potential sites for probes, a probe designated EP402-423 (5'-GAAAKGYGTCCATCCTCCACG-3'; K = G or T) was chosen based on the specificity experiment with rDNAs from many environmental clones and isolates as described below. For detection of the whole microbial population, the previously established probe UNI 522 was used (14). The MGI 391-413 and EP 402-423 sequences were analyzed with the Check Probe analysis from the RDP-II (25) and the gapped BLAST search algorithm (2, 5) to confirm the specificity of the probe for the rDNA sequences of the target microbial phylogroups. Based on in silico analysis, MGI 391-413 was found to bind specifically to MGI rRNA sequences and to have at least three bases of mismatch with any other archaeal rDNA sequences. EP 402-423 was also fully complementary to the epsilon-proteobacterial rRNA sequences in databases obtained from deep-sea hydrothermal environments at the probe-binding site, while many rRNA sequences from *Campylobacter* spp. had one mismatch and all other bacterial members had more than two mismatches with this probe.

In addition, dot-hybridization analysis was carried out with representative archaeal and bacterial rDNA clones obtained from both deep-sea hydrothermal systems (unpublished data) and various isolates of epsilon-*Proteobacteria* from the Central Indian Ridge Kairei field and the Okinawa Trough (49). The purified rDNAs (100 ng) amplified from the representative archaeal and bacterial rDNA clones were blotted onto positively charged nylon membranes (Roche Diagnostics) and cross-linked to the membranes by exposure to 120 mJ of UV light energy with a UV Stratalinker 1800 (Stratagene, Torrey Pines, Calif.). The membrane was hybridized with the MGI 391-413 and EP 402-423 probe (5 ng  $\mu$ l<sup>-1</sup>), which were labeled at the 5' end with digoxigenin and purified by high-pressure liquid chromatography (Amersham Pharmacia Biotech.). After hybridization, the membrane was washed, and the digoxigenin-labeled oligonucleotide probe hybridized with the targeted rDNA sequence was detected with the digoxi-

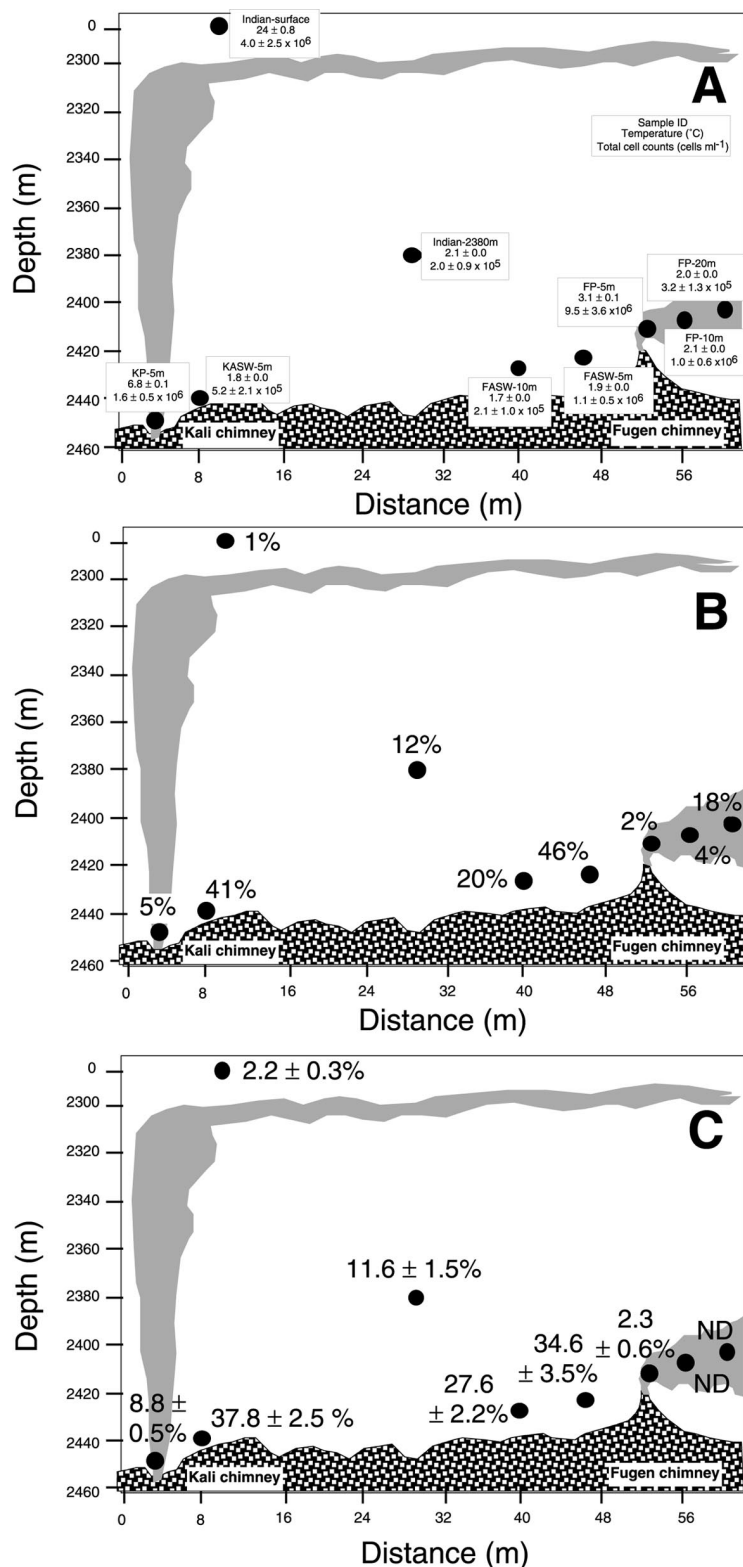


FIG. 1. Positions of water samples (A), proportion of MGI rDNA to the whole microbial rDNA assemblage (B), and proportion of MGI cells to the whole microbial community (C) in Kairei Field. The potential occurrence of hydrothermal plumes is indicated by gray shading. The depth of horizontally buoyed hydrothermal plumes was expected from the data obtained with a geochemical anomaly monitoring system. The data shown in B indicate the calculated proportion of MGI rDNA to whole microbial rDNA. The data shown in C indicate the proportion of MGI cells to whole microbial cells, determined by FISH analysis as in Table 2. ND, not determined.

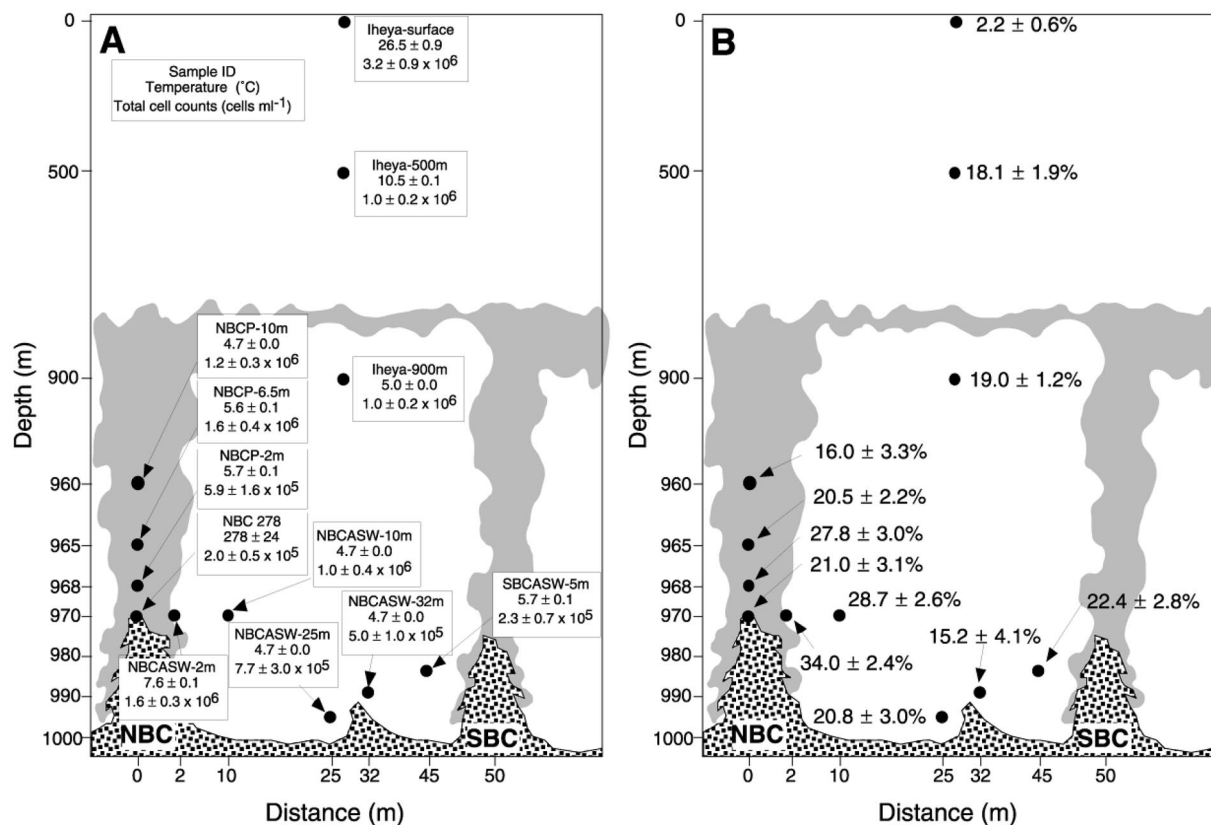


FIG. 2. Positions of water samples (A) and proportion of MGI cells to the whole microbial community (B) in Iheya North. The potential occurrence of hydrothermal plumes is indicated by gray shading. The data shown in B indicate the proportion of MGI cells to whole microbial cells, determined by FISH analysis as in Table 2.

genin luminescent detection kit for nucleic acids (Roche Diagnostics). All hybridization and washing procedures were carried out in the same conditions as described below. These experiments supported the specificity of each oligonucleotide probe for MGI and epsilon-*Proteobacteria* rDNA sequences.

For the whole-cell FISH experiment, the filter sample fixed with 3 ml of synthetic seawater containing 3.7% formaldehyde was dispersed by pipetting, and 1 ml of suspended seawater was centrifuged at  $10,000 \times g$  at 4°C. The cell pellet was washed with 0.5 ml of distilled, deionized water and centrifuged at  $10,000 \times g$  at 4°C again. The washed cells were stained with 60  $\mu$ l of distilled, deionized water containing DAPI ( $10 \mu\text{g ml}^{-1}$ ) overnight, and 20  $\mu$ l of each cell suspension was immobilized on a noncoated glass slide. Hybridization was performed with indocarbocyanine (Cy3)-labeled probes for 5 h in a hybridization buffer containing 30% formamide as previously described (46). The hybridization temperature was optimized for each probe as follows: MGI 391-413 probe, 48°C; EP 402-423 probe, 45°C; and UNI 522 probe, 42°C. After hybridization, the slide was washed at the same temperature used for hybridization for 2 h with hybridization buffer containing 35% formamide. Finally, the slide was examined under an Olympus BX51 epifluorescence microscope with the SPOT RT Slider charge-coupled device camera system (Diagnostic Instruments Inc.). Throughout the FISH experiment, it was estimated that approximately 30 to 50% of the total cells determined by direct filtering of the water sample were lost. This might have occurred during resuspension of the filter and centrifugation.

Two types of negative control experiments were employed with identical cell preparations and hybridization conditions. In one, the unlabeled MGI 391-413 and EP 402-423 probes were added in 50-fold excess ( $250 \text{ ng } \mu\text{l}^{-1}$ ) to the Cy3-labeled MGI 391-413 and EP 402-423 probes added at the standard concentration ( $5 \text{ ng } \mu\text{l}^{-1}$ ). In the other experiment, a Cy3-labeled negative (nonsense) probe identical to the probe in length and base composition was used. The sequences of the nonsense probes for MGI 391-413 and EP 402-423 were 5'-A ACCCGYACTGAAGTCGYTATA-3' and 5'-AAGGCTCCAGGAKYTACTC C-3', respectively. No microbial cells with clear Cy3-derived fluorescence signals were obtained, and the standard for manually identifying positive and negative hybridizations was established from both negative control experiments. Three

slides were prepared from each sample, and microbial cells in at least  $5 \times 10^{-7} \text{ m}^2$  on each slide were manually counted. Finally, an average of the ratio of probe-hybridized cells to DAPI-stained cells was determined from three slides.

**Nucleotide sequence accession number.** The 16S rDNA sequences of the rDNA clones described in this study were deposited in the DDBJ/EMBL/GenBank nucleotide sequence databases with accession numbers AB095113, AB095119, AB095135 to AB095137, and AB108843 to AB108849.

## RESULTS AND DISCUSSION

**Properties of the vent areas.** In the Kairei Field, the temperature of the ambient seawater was 1.7 to 1.9°C but decreased slightly with increasing distance from the hydrothermal emission and chimney (Fig. 1A). The plume waters had higher temperatures than the ambient seawaters, which was a good indication of mixing between hydrothermal emissions and seawater (Fig. 1A). In Iheya North, the average temperature of the ambient seawater distantly associated with hydrothermal activity was 4.7°C (Fig. 2A). However, the ambient seawater adjacent to the hydrothermal emissions and chimneys (samples NBCASW-2m and SBCASW-5m) was relatively warm ( $7.6 \pm 0.1^\circ\text{C}$  and  $5.7 \pm 0.1^\circ\text{C}$ , mean  $\pm$  standard deviation, respectively) (Fig. 2A). The difference in the temperature profiles of the ambient seawater was likely associated with different modes of hydrothermal fluid emission between the Kairei Field and the Iheya North systems. The hydrothermal emission in the Kairei Field was very vigorous and occurred intensively in the vent orifice and assemblages of chimney

structures (height, 2 to 5 m; maximum height, 10 m), while most of the hydrothermal emissions in Iheya North were diffusive flows from many parts of the large mounds (height, 30 to 40 m) containing flange structures (24). It seemed likely that the ambient seawater close to the hydrothermal mounds was influenced by the diffusive emissions from the bottom parts of the mound structures.

**Total cell counts.** The normal deep seawater had  $2.0 \times 10^5 \pm 0.9 \times 10^5$  cells  $\text{ml}^{-1}$  ( $\pm$  standard deviation) (Indian-2380m),  $1.0 \times 10^6 \pm 0.2 \times 10^6$  cells  $\text{ml}^{-1}$  (Iheya-900m), and  $1.0 \times 10^6 \pm 0.2 \times 10^6$  cells  $\text{ml}^{-1}$  (Iheya-500m) (Fig. 1A and 2A). Compared to these microbial community densities, the ambient seawater just adjacent to hydrothermal emissions (samples KASW-5m, FASW-5m, and NBCASW-2m) contained slightly higher densities ( $5.2 \times 10^5 \pm 2.1 \times 10^5$ ,  $1.1 \times 10^6 \pm 0.5 \times 10^6$ , and  $1.6 \times 10^6 \pm 0.3 \times 10^6$  cells  $\text{ml}^{-1}$ , respectively) (Fig. 1A and 2A) but the ambient seawater distantly located from the deep-sea hydrothermal vents (FASW-10m, NBCASW-25m, and NBCASW-32m) had similar and lower densities ( $2.1 \times 10^5 \pm 1.0 \times 10^5$ ,  $7.7 \times 10^5 \pm 3.0 \times 10^5$ , and  $5.0 \times 10^5 \pm 1.0 \times 10^5$  cells  $\text{ml}^{-1}$ , respectively) than the normal deep seawaters (Fig. 1A and 2A).

The greatest microbial community density was obtained in the hydrothermal plumes; the density was greater in plume water closer to the vents in the Kairei Field ( $1.6 \times 10^6 \pm 0.5 \times 10^6$  cells  $\text{ml}^{-1}$  for KP-5m and  $9.5 \times 10^6 \pm 3.6 \times 10^6$  cells  $\text{ml}^{-1}$  for FP-5m), while the plume water 5 to 10 m from the vent ( $1.6 \times 10^6 \pm 0.4 \times 10^6$  cells  $\text{ml}^{-1}$  for NBCP-6.5m and  $1.2 \times 10^6 \pm 0.3 \times 10^6$  cells  $\text{ml}^{-1}$  for NBCP-10m) harbored larger populations than the plume water at 2 m ( $5.9 \times 10^5 \pm 1.6 \times 10^5$  cells  $\text{ml}^{-1}$  for NBCP-2m) in Iheya North (Fig. 1A and 2A).

The microbial community density obtained from both deep-sea hydrothermal systems and the water columns above the hydrothermal activities were considerably higher than previously determined densities of the vertically distributed microbial communities in the tropical to subtropical Indian and Pacific oceans (9, 10, 19, 32). From the northwestern Indian Ocean ( $0^\circ\text{N}$  to  $22^\circ\text{N}$ ),  $0.5 \times 10^6$  to  $>1.5 \times 10^6$  cells  $\text{ml}^{-1}$  (9) and  $0.8 \times 10^6$  to  $1.4 \times 10^6$  cells  $\text{ml}^{-1}$  (10) were reported as the microbial community densities in the surface water and  $<0.5 \times 10^5$  to  $1.0 \times 10^5$  cells  $\text{ml}^{-1}$  (10) was the microbial community density at a depth zone of 2,000 to 3,000 m (9). Similarly, in the Pacific, the surface microbial community density varied from  $0.4 \times 10^6$  to  $4.0 \times 10^6$  cells  $\text{ml}^{-1}$  but was lower in the subtropical than in the subarctic region (32). The deep-sea waters (1,000 to 4,000 m) in the subtropical regions had a microbial community density of  $1.0 \times 10^4$  to  $9.0 \times 10^4$  cells  $\text{ml}^{-1}$  (32). A whole-cell FISH-mediated estimate provided much lower values than  $2 \times 10^4$  cells  $\text{ml}^{-1}$  below 1,000 m in the subtropical Pacific (19).

Although the comparison with the previous investigations on the bacterioplankton density suggests possible overestimation of the microbial community density in this study, a higher density in both of the deep-sea hydrothermal sites and their vicinities may represent a higher productivity of the bacterioplanktonic population. As pointed out in the previous investigations of the distribution and abundance of various bacterioplankton (9, 10, 32, 34), the seasonal and geographical alterations in the abundance and productivity of the surface and deep-seawater microbial communities were strongly asso-

ciated with different physical and geochemical settings. The hydrothermal activity in the deep ocean floor might have significant physical and geochemical impacts on the vicinity and even on the water column above. The hydrothermal plume is one of the most outstanding phenomena, and its influence is known to reach several hundred meters to several kilometers vertically and several to 10 kilometers horizontally around the site despite no apparent temperature anomaly (25). In addition, the mode and magnitude of the hydrothermal activity may affect the spatial profile of microbial community density. The different distribution profiles of microbial community density in two deep-sea hydrothermal systems reflect the different physical and geochemical backgrounds.

**Phylotype distribution in the planktonic habitats.** The proportion of archaeal rDNA in the whole microbial DNA assemblage determined by quantitative fluorescent PCR varied among the samples. The plume waters (samples KP-5m, FP-5m, FP-10m, and FP-20m) had relatively low proportions of archaeal rDNA populations (6, 4, 5, and 20%, respectively). The archaeal rDNA proportion was increased and the archaeal phylotype structure was shifted in the Fugen Chimney plume with increasing distance from the vent. The nearest plume water contained a number of hyperthermophilic archaeal components related to the *Methanopyrales* and *Thermococcales* (Fig. 3 and Table 1). In the distant plume water, the proportion of archaeal phylotypes associated with MGI was increased (Fig. 3 and Table 1). In contrast, the archaeal rDNA communities in the ambient seawater consisted only of MGI members (Fig. 3 and Table 1), and the proportions of archaeal rDNA in the whole microbial DNA assemblages (48% in KASW-5m, 45% in FASW-5m, and 20% in FASW-10m) were higher than in the normal deep and surface seawater (13% in Indian-2380m and 9% in Indian-surface) as well as in the plume waters. The highest proportion of archaeal rDNA was obtained from the ambient seawater just adjacent to hydrothermal emissions and chimneys.

The archaeal rDNA community in the surface water was quite different from that in the deep-sea hydrothermal ambient seawater and normal deep seawater, and it contained a high abundance of marine euryarchaeota group II (MGII) (Fig. 3 and Table 1). The predominant occurrence of MGII members in the surface and shallower zones of the ocean was previously demonstrated by Massana et al. (29), and the results in this study might represent a vertical shift in the archaeal rDNA community structures in the Kairei Field, Indian Ocean, at the time of sampling. In addition, phylogenetic analysis of the MGI phylotypes obtained from the deep-sea hydrothermal environments, including the Kairei Field and other oceanic habitats, revealed the distribution of different phylotypes of MGI in different oceanic habitats (Fig. 3).

Massana et al. (29) also demonstrated the phylogenetic taxonomy (MGI- $\alpha$ , - $\beta$ , and - $\gamma$ ) of a number of MGI rDNA sequences recovered from a variety of geographical regions and depths of marine environments and suggested that the phylotypes within MGI- $\alpha$  dominated the planktonic archaeal population in the shallow waters, whereas MGI- $\gamma$  contained the phylotypes obtained from deep waters. The predominant MGI rDNA clone (pCIRA-ZI) from the Kairei Field was affiliated within the MGI- $\gamma$  with most of the deep-sea hydrothermal vent MGI rDNA clones from other fields (Fig. 3) (31, 47). The

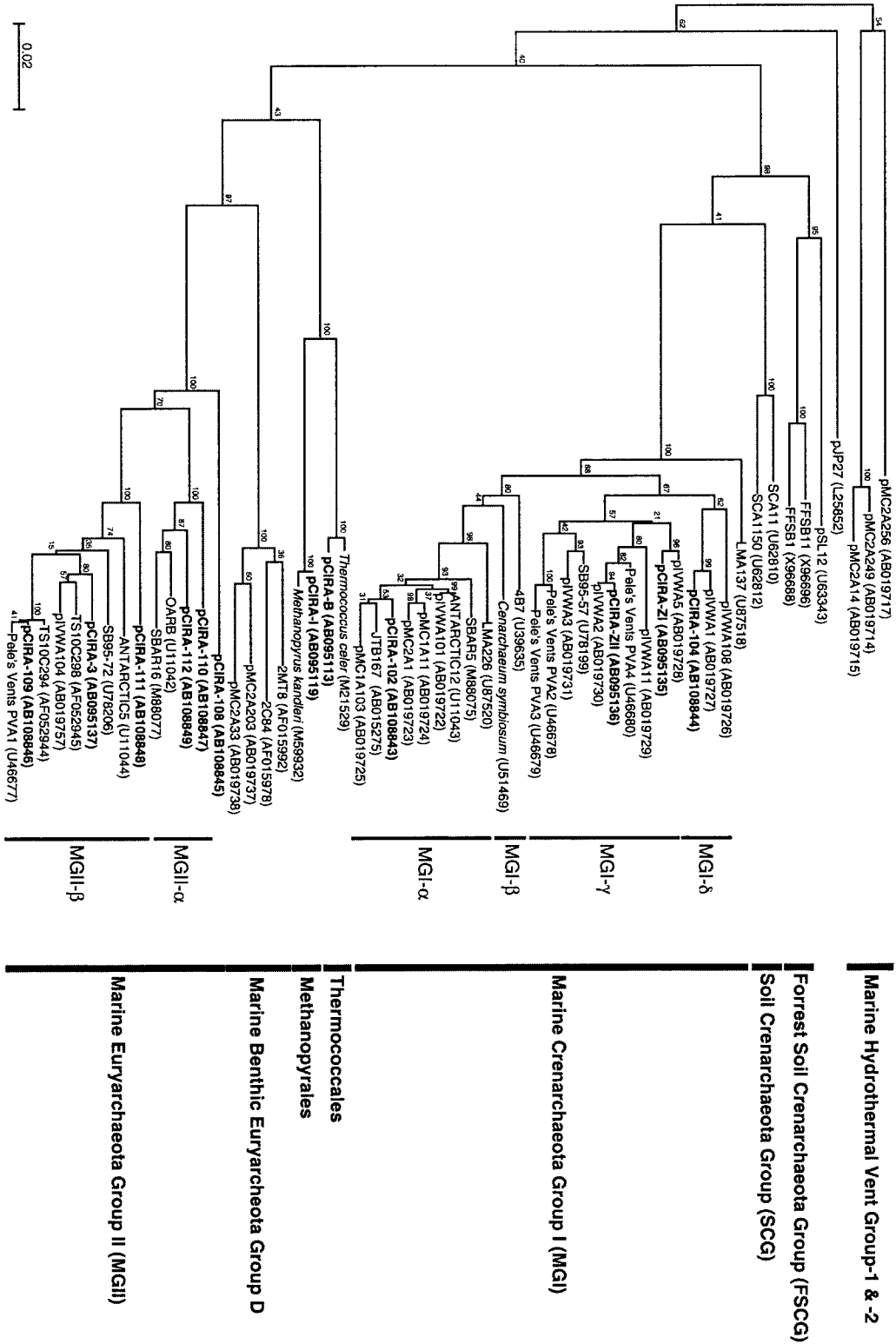


FIG. 3. Phylogenetic tree of representative archaeal phylogenotypes obtained from water samples in Kairei Field. The tree was constructed by neighbor-joining analysis of 669 homologous positions of the rDNA sequence. Bold indicates rDNA clones obtained from Kairei Field. The classification of subgroups within MGI and MGII was that of Massana et al. (28). Bootstrap analysis was performed with 100 resampled data sets. The bar indicates 0.02 change per nucleotide.

TABLE 1. Representative archaeal rDNA clones and the archaeal rDNA community structure of each water sample from the Kairei deep-sea hydrothermal field

Group and representative rDNA clone	Similar sequence (% similarity) <sup>a</sup>	No. of clones obtained from sample:								
		FP-5m	KP-5m	FP-10m	FP-25m	FASW-5m	KASW-5m	FASW-10m	Indian-2380m	Indian-surface
<i>Methanopyrales</i>										
pCIRA-I	<i>Methanopyrus kandleri</i> (98.3)	14		2						
<i>Thermococcales</i>										
pCIRA-B	<i>Thermococcus celer</i> (98.3)		2	1						
MGI										
pCIRA-ZI	DHVE clone pIVWA5 (98.7)	6	16	10	43	20	22	16	19	1
pCIRA-ZII	DHVE clone pIVWA2 (99.7)		1	3					1	
pCIRA-102	DHVE clone pIVWA101 (98.2)	5							1	
pCIRA-104	DHVE clone pIVWA1 (99.4)		1							
MGI										
pCIRA-3	Fish clone TS10C294 (94.3)		1	1	5				1	
pCIRA-108	Fish clone TS10C294 (84.9)								1	
pCIRA-109	Fish clone TS10C294 (99.3)									14
pCIRA-110	Planktonic clone OARB (94.5)									7
pCIRA-111	Planktonic clone SBAR16 (88.2)									1
pCIRA112	Planktonic clone OARB (94.6)									1
Total		25	21	17	48	20	22	16	23	27

<sup>a</sup> DHVE, deep-sea hydrothermal vent.

phylogenetic relatedness between the deep-sea hydrothermal vent MGI members and deep-sea planktonic ones may provide an important clue to identifying the source and sink of the abundantly and ubiquitously distributed MGI population in the global oceanic biosphere.

On the basis of the results from the archaeal rDNA clone analysis and quantitative PCR, the proportion of MGI rDNA clone types in the whole microbial rDNA community was calculated as follows: (i) the proportion of the rDNA clones phylogenetically associated with MGI in the archaeal rDNA clone library from each sample was calculated, and (ii) the proportion of MGI rDNA clone types in the archaeal rDNA clone library was multiplied by the proportion of archaeal rDNA determined by quantitative PCR. The proportion of MGI rDNA clone types in the whole microbial rDNA community was based on the PCR-mediated analysis and did not properly represent the proportion of MGI cells in the whole microbial community. However, the sketch for the abundance of MGI rDNA in the whole microbial rDNA assemblage would provide an important insight into the spatial distribution profile of MGI rDNAs and cells in the vicinity of the deep-sea hydrothermal system. A scheme representing a spatial distribution profile of MGI rDNAs in the whole microbial rDNA assemblage is shown in Fig. 1B. The patchy distribution of MGI rDNA was evident in the vicinity of the Kairei deep-sea hydrothermal field (Fig. 1B). The highest proportion of MGI rDNA in the whole microbial rDNA community was observed in the ambient seawater just adjacent to hydrothermal emissions and chimneys (Fig. 1B).

**Analysis via whole-cell fluorescence hybridization.** Based on the recent culture-independent molecular surveys, it has been suggested that both MGI and epsilon-*Proteobacteria* are the most abundant microbial components in the relatively low temperatures of habitats in the deep-sea hydrothermal environments (45, 49).

The proportion of MGI 391-413, EP 402-423, and UNI 522 probe-binding cells to DAPI-stained cells is summarized in Table 2. The proportion of the universal probe-binding cells to

DAPI-stained cells was significantly higher on the whole in this study than determined previously in the planktonic microbial communities with more sensitive polynucleotide probes (19). One possible reason for the high proportion of universal-probe-binding cells to DAPI-stained cells in this study is that the proportion of universal-probe-binding cells was determined against the total number of cells stained by DAPI prior

TABLE 2. Proportion of DAPI-stained microbial cells binding an MGI-specific, epsilon-*Proteobacteria*-specific, or universal probe

Sample	Proportion to DAPI-stained cells (%) ± SD binding to probe:		
	MGI 391-413	EP 402-423	UNI 522
Hydrothermal emission			
NBC 278°C	21.0 ± 3.1	22.5 ± 3.8	88.7 ± 18.9
Hydrothermal plume			
Avg	16.7 ± 9.3	23.0 ± 8.9	117 ± 24.4
KP-5m	8.8 ± 0.5	12.3 ± 1.7	110 ± 16.0
FP-5m	2.3 ± 0.6	9.4 ± 0.6	122 ± 30.8
NBCP-2m	27.8 ± 3.0	21 ± 3.1	107 ± 24.1
NBCP-6.5m	20.5 ± 2.2	31.9 ± 3.2	128 ± 33.4
NBCP-10m	16 ± 3.3	29.8 ± 4.0	119 ± 17.5
Ambient seawater			
Avg	26.2 ± 6.6	7.1 ± 5.1	80.2 ± 23.1
KASW-5m	37.8 ± 2.5	5.3 ± 2.2	85.2 ± 20.7
FASW-5m	34.6 ± 3.5	4.8 ± 2.0	83.3 ± 31.1
FASW-10m	27.6 ± 2.2	2.5 ± 1.1	76.9 ± 22.2
NBCASW-2m	34 ± 2.4	10.5 ± 2.8	83.6 ± 15.8
NBCASW-10m	28.7 ± 2.6	15.8 ± 3.8	75.7 ± 27.2
NBCASW-25m	20.8 ± 3.0	2.1 ± 0.9	72.1 ± 12.5
NBCASW-32m	15.2 ± 4.1	2.5 ± 0.5	77.4 ± 20.6
SBCASW-5m	22.4 ± 2.8	11.5 ± 3.5	87.5 ± 35.0
Deep seawater			
Avg	18.6 ± 0.5	0.5 ± 0.5	80.4 ± 15.6
Indian-2380m	11.6 ± 1.5	0.2 ± 0.1	79.5 ± 16.6
Iheya-900m	19 ± 1.2	1.0 ± 0.6	73.3 ± 19.8
Iheya-500m	18.1 ± 1.9	0	88.5 ± 10.9
Surface seawater			
Avg	2.2	0	98.2 ± 17.7
Indian-surface	2.2 ± 0.3	0	99.1 ± 15.5
Iheya-surface	2.2 ± 0.6	0	97.2 ± 19.9

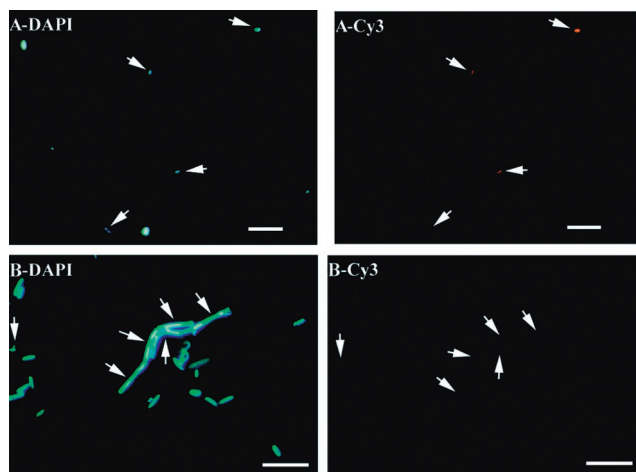


FIG. 4. Whole-cell FISH analysis with a Cy3-labeled, MGI-specific probe (MGI 391-413) (A) or epsilon-*Proteobacteria*-specific probe (EP 402-423) (B) and DAPI as a counterstain (A and B). (A) Photographs of microbial cells stained with DAPI (A-DAPI) and binding the MGI-specific probe (A-Cy3) in sample FASW-5m. (B) Photographs of microbial cells stained with DAPI (B-DAPI) and binding the epsilon-*Proteobacteria*-specific probe (B-Cy3) in sample NBCP-6.5m. Arrows indicate MGI cells (A) and epsilon-proteobacterial cells (B). Bars, 10  $\mu\text{m}$  (A) and 5  $\mu\text{m}$  (B).

to hybridization. Thus, the DAPI-stained cell count performed simultaneously with FISH analysis was likely an underestimate compared to the cell count obtained when DAPI staining was done just before the microscopic observation. When we evaluated the extent of the underestimation by experiments with representative samples (KP-5m, NBCP-6.5, FASW-5m, NBCASW-25m, Indian-2380m, Iheya-500m, and Indian-surface), in which the samples on the slides stained with DAPI were counted in the presence and absence of the hybridization procedure without any of probes, on average 15% of the DAPI-stained cells were destined (maximally 30%) during the hybridization procedure. This result suggested that the proportion of universal-probe-binding cells to DAPI-stained cells might have been overestimated in this study. Despite the possible overestimation of the proportion of universal-probe-binding cells, a relatively higher proportion of universal-probe-binding cells was always obtained from the surface seawater microbial communities and the plume water communities (Table 2). These results may represent the higher proportion of metabolically active cells in the plume water and surface seawater than in ambient and normal deep seawater.

The spatial distribution profiles of MGI cells in the Kairei Field and Iheya North were sketched based on the results from FISH analysis (Fig. 1C, 2B, and 4A). As demonstrated in the case of the Kairei Field by rDNA abundance with PCR-mediated methods, a patchy distribution of MGI members was evident by FISH analysis in the vicinity of the Kairei deep-sea hydrothermal field, and the prevalent occurrence of MGI in the ambient seawaters just adjacent to hydrothermal emissions and chimneys was indicated (Fig. 1C). In addition, a very similar profile of MGI distribution was obtained from FISH analysis in case of Iheya North (Fig. 2B). With the values on the proportion of MGI rDNA clone types in the whole microbial rDNA community obtained from the PCR-mediated anal-

ysis (Fig. 1B) and on the proportion of MGI cells in the whole microbial community obtained from FISH analysis (Fig. 1C), a correlation between two independent analyses targeting different molecules was estimated. The linear regression slope was 0.78 (95% confidence interval, 0.73 to 1.27,  $n = 7$ ), and the correlation coefficient ( $r^2$ ) was 0.957 for the two methods. This estimate revealed that the two molecular analyses determining the distribution of MGI were significantly correlated in the samples from Kairei Field. Thus, based on the different estimation methods and in both Kairei Field and Iheya North, MGI members increased their proportion in the ambient seawater habitats close to hydrothermal emissions and chimneys. Finally, the distribution profile of epsilon-*Proteobacteria* differed from that of MGI cells (Table 2). The highest proportion of epsilon-*Proteobacteria* in the whole microbial community was detected in plume water in Kairei Field and Iheya North, and the average proportion of epsilon-*Proteobacteria* in plume water was three times as high as that in the ambient seawater (Table 2). In addition, the plume water samples had many dividing and aggregating form of cells that bound to the EP 402-423 probe (Fig. 4B).

**Implications of the distribution profile of MGI.** On the basis of a molecular phylogenetic survey of archaeal components in microbial mats at Pele's Vents, Loihi Seamount, Hawaii, Moyer et al. hypothesized that deep-sea hydrothermal systems were potential sources and sinks of marine planktonic *Archaea* (31). In this study, the proportion of MGI members was apparently higher in the ambient seawater than in the normal deep seawater in the geographically and geologically distinct deep-sea hydrothermal systems (Table 2). Several investigations have suggested that the deep ocean below the euphotic zone has a higher population of MGI than the surface and is a potential niche for MGI members (7, 19, 29). In addition, it was clearly demonstrated in this study that the MGI members dominating the planktonic microbial communities in deep-sea hydrothermal environments are phylogenetically associated with the deep-ocean MGI members rather than the shallow-water entities. Hence, the ambient seawater habitats of the deep-sea hydrothermal sites may represent a suitable habitat for some groups of MGI and may be a possible source environment of them.

In comparison to the distribution profiles of another major constituent of the *Bacteria* in the low-temperature habitats of deep-sea hydrothermal environments, potentially chemolithoautotrophic epsilon-*Proteobacteria*, the uncultivated MGI members exhibited a different distribution, implying that the deep-sea hydrothermal vent MGI members were not as fully dependent on chemolithoautotrophic metabolism as epsilon-*Proteobacteria*. Our recent cultivation and characterization of many previously uncultivated epsilon-*Proteobacteria* inhabiting a variety of deep-sea hydrothermal habitats demonstrated that most were anaerobic to microaerobic, strictly chemolithoautotrophic, hydrogen- and/or sulfur-oxidizing microorganisms (49). These currently characterized physiological and metabolic features of the deep-sea hydrothermal vent epsilon-*Proteobacteria* could well explain the distribution profile of epsilon-*Proteobacteria* in plume water in relation to the abundance and utilization of energy sources such as hydrogen and reduced sulfur compounds. This adversely implies that most MGI members predominantly occurring in the ambient seawater have

physiological and metabolic traits that differ from those of deep-sea hydrothermal vent epsilon-*Proteobacteria* and may be not chemolithoautotrophs, which has been suggested by recent investigations of environmental archaeal lipids, isotopic carbon characterization of the lipid components and an in situ tracer experiment with a stable carbon isotope (15, 21, 22, 35, 42, 43, 58).

Despite extensive and comparative characterization of hydrothermal vent fluids in global deep-sea hydrothermal systems (57), the physical and chemical properties of the water in the vicinity of the deep-sea hydrothermal systems have been poorly investigated other than in large hydrothermal plumes (25). Much less is known about the physical and chemical properties of ambient seawater at high resolution. A distinctive feature, apparently found in the ambient environments of hydrothermal emissions and chimneys, is the formation of prosperous macrofaunal communities. In Kaiei Field and Iheya North, a number of animal communities consisting of vent mussels (both locations), crabs (both locations), arthropods (both locations), polychaetes (both), tubeworms (Iheya North), and shrimps (Kaiei Field) were observed widely at the surface and the foot of the chimney structures. These animal communities might excrete considerable amounts of dissolved organic compounds into the ambient seawater.

Although geochemical characterization of dissolved organic compounds in the water samples was not conducted in this study, organic compounds derived from the deep-sea hydrothermal animal communities may have a great impact on the energy and carbon metabolisms of the microorganisms in the vicinity of deep-sea hydrothermal systems. Biochemical signatures for heterotrophic metabolism of MGI members have been obtained from substrate-tracking autoradiography fluorescence in situ hybridization experiments by Ouverney and Fuhrmann (33). Recent genomic investigations of several phylotypes of MGI with large DNA fragments directly recovered from such environments have revealed a diversity of genes and genomic structures within MGI members and may allow the physiological and metabolic diversity and speciation of MGI in a variety of oceanic habitats (3, 4, 40, 44). Further investigation with a combination of molecular phylogenetic techniques and isotopic characterization of MGI lipids will provide an important clue to understanding the physiological and metabolic traits of the deep-sea hydrothermal vent MGI members and lead to future successful cultivation of what is potentially the largest population of *Archaea* on this planet.

#### ACKNOWLEDGMENTS

We are very grateful to the crews of the R/Vs *Natsushima* and *Yokosuka* and the operating teams of DSVs *Shinkai 2000* and *Shinkai 6500* for helping us to collect deep-sea hydrothermal vent samples.

#### REFERENCES

- Alain, K., J. Querellou, F. Lesongeur, P. Pignet, P. Crassous, G. Ragueneas, V. Cuff, and M.-A. Cambon-Bonavita. 2002. *Caminibacter hydrogeniphilus* gen. nov., sp. nov., a novel thermophilic, hydrogen-oxidizing bacterium isolated from an East Pacific Rise hydrothermal vent. *Int. J. Syst. Evol. Microbiol.* **52**:1317–1323.
- Altschul, S. F., T. L. Madden, A. A. Schäffer, J. Zhang, Z. Zhang, W. Miller, and D. J. Lipman. 1997. Gapped BLAST and PSI-BLAST: a new generation of protein database search programs. *Nucleic Acids Res.* **25**:3389–3402.
- Beja, O., M. T. Suzuki, E. V. Koonin, L. Aravind, A. Hadd, L. P. Nguyen, R. Villacorta, M. Amjadi, C. Garrigues, S. B. Jovanovich, R. A. Feldman, and E. F. DeLong. 2000. Construction and analysis of bacterial artificial chromo-
- some libraries from a marine microbial assemblage. *Environ. Microbiol.* **2**:516–529.
- Beja, O., E. V. Koonin, L. Aravind, L. T. Taylor, H. Seitz, J. L. Stein, D. C. Bensen, R. A. Feldman, R. V. Swanson, and E. F. DeLong. 2002. Comparative genomic analysis of archaeal genotypic variants in a single population and in two different oceanic provinces. *Appl. Environ. Microbiol.* **68**:335–345.
- Benson, D. A., M. S. Boguski, D. J. Lipman, J. Ostell, and B. F. F. Ouellette. 1998. Genbank. *Nucleic Acids Res.* **26**:1–7.
- DeLong, E. F. 1992. *Archaea* in coastal marine environments. *Proc. Natl. Acad. Sci. USA* **89**:5685–5689.
- DeLong, E. F., K. Y. Wu, B. B. Prezelin, and R. V. M. Jovine. 1994. High abundance of *Archaea* in Antarctic marine picoplankton. *Nature* **371**:695–697.
- DeLong, E. F., L. T. Taylor, T. L. Marsh, and C. M. Preston. 1999. Visualization and enumeration of marine planktonic *Archaea* and *Bacteria* by using polyribonucleotide probes and fluorescence in situ hybridization. *Appl. Environ. Microbiol.* **65**:5554–5563.
- Ducklow, H. W. 1993. Bacterioplankton distribution and production in the northwestern Indian Ocean and Gulf of Oman, September 1986. *Deep-Sea Res. II* **40**:753–771.
- Ducklow, H. W., D. C. Smith, L. Camobell, M. R. Landry, H. L. Quinby, G. F. Steward, and F. Azam. 2001. Heterotrophic bacterioplankton in the Arabian Sea: basin wide response to year-round high primary productivity. *Deep-Sea Res. II* **48**:1303–1323.
- Fuhrman, J. A., K. McCallum, and A. A. Davis. 1992. Novel major archaeobacterial group from marine plankton. *Nature* **356**:148–149.
- Fuhrman, J. A., and A. A. Davis. 1997. Widespread archaea and novel bacteria from the deep sea as shown by 16S rRNA gene sequences. *Mar. Ecol. Prog. Ser.* **150**:275–285.
- Gamo, T., K. Okamura, J.-L. Charlou, T. Urabe, J.-M. Auzende, J. Ishibashi, K. Shitashima, H. Chiba, and Shipboard Scientific Party of the Manus Flux Cruise. 1997. Acidic and sulfate-rich hydrothermal fluids from the Manus back-arc basin, Papua New Guinea. *Geology* **25**:139–142.
- Giovannoni, S. J., E. F. DeLong, G. J. Olsen, and N. R. Pace. 1988. Phylogenetic group-specific oligonucleotide probes for identification of single microbial cells. *J. Bacteriol.* **170**:720–726.
- Hoefs, M. J. L., S. Shouten, J. W. De Leeuw, L. L. King, S. G. Wakeham, and J. S. Sinninghe Damste. 1997. Ether lipids of planktonic archaea in the marine water column. *Appl. Environ. Microbiol.* **63**:3090–3095.
- Inagaki, F., K. Takai, T. Komatsu, T. Kanamatsu, K. Fujioka, and K. Horikoshi. 2001. Archaeology of *Archaea*: geomicrobiological record of Pleistocene thermal events concealed in a deep-sea seafloor environment. *Extremophiles* **5**:385–392.
- Inagaki, F., K. Takai, T. Komatsu, Y. Sakihama, A. Inoue, and K. Horikoshi. 2002. Profile of microbial community structure and presence of endolithic microorganisms inside a deep-sea rock. *Geomicrobiol. J.* **19**:535–552.
- Karner, M., and J. A. Fuhrman. 1997. Determination of active marine bacterioplankton: a comparison of universal 16S rRNA probes autoradiography, and nucleoid staining. *Appl. Environ. Microbiol.* **63**:1208–1213.
- Karner, M. B., E. F. DeLong, and D. M. Karl. 2001. Archaeal dominance in the mesopelagic zone of the Pacific Ocean. *Nature* **409**:507–510.
- Kato, C., L. Li, J. Tamaoka, and K. Horikoshi. 1997. Molecular analyses of the sediment of the 11000-m deep Mariana Trench. *Extremophiles* **1**:117–123.
- Kuypers, M. M. M., P. Blokker, J. Erbacher, H. Kinkel, R. D. Pancost, and S. Shouten, and J. S. Sinninghe Damste. 2001. Massive expansion of marine *Archaea* during a mid-Cretaceous oceanic anoxic event. *Science* **293**:92–94.
- Kuypers, M. M. M., P. Blokker, E. C. Hopmans, H. Kinkel, R. D. Pancost, and S. Shouten, and J. S. Sinninghe Damste. 2002. Archaeal remains dominate marine organic matter from the early Albian oceanic anoxic event 1b. *Paleogeogr. Paleoclimatol. Paleocool.* **185**:211–234.
- Lane, D. J. 1985. 16S/23S sequencing, p. 115–176. *In* E. Stackbrandt and M. Goodfellow (ed.), *Nucleic acid techniques in bacterial systematics*. John Wiley & Sons, New York, N.Y.
- Lonsdale, P., and K. Becker. 1985. Hydrothermal plumes, hot springs and conductive heat flow in the Southern Trough of Guaymas Basin. *Earth Planet. Sci. Lett.* **73**:211–225.
- Lupton, J. E. 1995. Hydrothermal plumes: near and far field, p. 317–346. *In* S. E. Humphris, R. A. Zierenberg, L. S. Mullineaux, and R. E. Tompson (ed.), *Geophysical monograph 91: seafloor hydrothermal system*. American Geophysical Union, Washington, D.C.
- MacGregor, B. J., D. P. Moser, E. W. Alm, K. H. Nealson, and D. A. Stahl. 1997. Crenarchaeota in Lake Michigan sediment. *Appl. Environ. Microbiol.* **63**:1178–1181.
- Maidak, B. L., J. R. Cole, T. G. Lilburn, C. T. Parker Jr., P. R. Saxman, J. M. Stredwick, G. M. Garrity, B. Li, G. J. Olsen, S. Pramanik, T. M. Schmidt, and J. M. Tiedje. 2000. The RDP (Ribosomal Database Project) continues. *Nucleic Acids Res.* **28**:173–174.
- Massana, R., A. E. Murray, C. M. Preston, and E. F. DeLong. 1997. Vertical distribution and phylogenetic characterization of marine planktonic archaea in the Santa Barbara Channel. *Appl. Environ. Microbiol.* **63**:50–56.

29. Massana, R., E. F. DeLong, and C. Pedros-Alio. 2000. A few cosmopolitan phylotypes dominate planktonic archaeal assemblages in widely different oceanic provinces. *Appl. Environ. Microbiol.* **66**:1777–1787.
30. Miroshnichenko, M. L., N. A. Kostrikina, S. L'Haridon, C. Jeannot, H. Hippe, E. Stackebrandt, and E. A. Bonch-Osmolovskaya. 2002. *Nautilia lithotrophica* gen. nov., sp. nov., a thermophilic sulfur-reducing  $\epsilon$ -Proteobacterium isolated from a deep-sea hydrothermal vent. *Int. J. Syst. Evol. Microbiol.* **52**:1299–1304.
31. Moyer, C. L., J. M. Tiedje, F. C. Dobbs, and D. M. Karl. 1998. Diversity of deep-sea hydrothermal vent archaea from Loihi Seamount, Hawaii. *Deep-Sea Res.* **45**:303–317.
32. Nagata, T., H. Fukuda, R. Fukuda, and I. Koike. 2000. Bacterioplankton distribution and production in deep Pacific waters: large-scale geographic variations and possible coupling with sinking particle fluxes. *Limnol. Oceanogr.* **45**:426–435.
33. Ouverney, C. C., and J. A. Fuhrman. 2000. Marine planktonic archaea take up amino acids. *Appl. Environ. Microbiol.* **66**:4829–4833.
34. Patching, J. W., and D. Eardly. 1997. Bacterial biomass and activity in the deep waters of the eastern Atlantic—evidence of a barophilic community. *Deep-Sea Res.* **44**:1655–1670.
35. Pearson, A., A. P. McNichol, B. C. Benitez-Nelson, J. M. Hayes, and T. I. Eglinton. 2001. Origins of lipid biomarkers in Santa Monica Basin surface sediments: a case study using compound-specific  $^{14}\text{C}$  analysis. *Geochim. Cosmochim. Acta* **65**:3123–3137.
36. Preston, C. M., K. Y. Wu, T. F. Molinski, and E. F. DeLong. 1996. A psychrophilic crenarchaeon inhabits a marine sponge: *Cenarchaeum symbiosum* gen. nov., sp. nov. *Proc. Natl. Acad. Sci. USA* **93**:6241–6246.
37. Sakai, H., T. Gamo, E.-S. Kim, K. Shitashima, F. Yanagisawa, and M. Tsutsumi. 1990. Unique chemistry of the hydrothermal solution in the mid-Okinawa trough backarc basin. *Geophys. Res. Lett.* **17**:2133–2136.
38. Sako, Y., K. Takai, Y. Ishida, A. Uchida, and Y. Katayama. 1996. *Rhodothermus obamensis* sp. nov., a modern lineage of extremely thermophilic marine bacteria. *Int. J. Syst. Bacteriol.* **46**:1099–1104.
39. Schleper, C., W. Holben, and H.-P. Klenk. 1997. Recovery of crenarchaeotal ribosomal DNA sequences from freshwater-lake sediments. *Appl. Environ. Microbiol.* **63**:321–323.
40. Schleper, C., R. V. Swanson, E. J. Mathur, and E. F. DeLong. 1997. Characterization of a DNA polymerase from uncultivated psychrophilic archaeon *Cenarchaeum symbiosum*. *J. Bacteriol.* **179**:7803–7811.
41. Shouten, S., M. J. L. Hoefs, M. P. Koopman, H.-J. Bosch, and J. S. Sinninghe Damste. 1998. Structural characterization, occurrence and fate of archaeal ether-bound acyclic and cyclic biphytanes and corresponding diols in sediments. *Org. Geochem.* **29**:1305–1319.
42. Shouten, S., E. C. Hopmans, R. D. Pancost, and J. S. Sinninghe Damste. 2000. Widespread occurrence of structurally diverse tetraether membrane lipids: evidence for the ubiquitous presence of low-temperature relatives of hyperthermophiles. *Proc. Natl. Acad. Sci. USA* **97**:14421–14426.
43. Sinninghe Damste, J. S., W. I. C. Rijpstra, E. C. Hopman, F. G. Prahl, and S. Schouten. 2002. Distribution of membrane lipids of planktonic crenarchaeota in the Arabian Sea. *Appl. Environ. Microbiol.* **68**:2997–3002.
44. Stein, J. L., T. L. Marsh, K. Y. Wu, H. Shizuya, and E. F. DeLong. 1996. Characterization of uncultivated prokaryotes: isolation and analysis of 40-kilobase-pair genome fragment from a planktonic marine archaeon. *J. Bacteriol.* **178**:591–599.
45. Takai, K., and Y. Fujiwara. 2002. Hydrothermal vents: biodiversity in deep-sea hydrothermal vents, p. 1604–1617. *In* G. Bitton (ed.), *Encyclopedia of environmental microbiology*. John Wiley & Sons, New York, N.Y.
46. Takai, K., and K. Horikoshi. 1999. Genetic diversity of archaea in deep-sea hydrothermal vent environments. *Genetics* **152**:1285–1297.
47. Takai, K., and K. Horikoshi. 2000. Rapid detection and quantification of members of the archaeal community by quantitative PCR using fluorogenic probes. *Appl. Environ. Microbiol.* **66**:5066–5072.
48. Takai, K., and Y. Sako. 1999. A molecular view of archaeal diversity in marine and terrestrial hot water environments. *FEMS Microbiol. Ecol.* **28**:177–188.
49. Takai, K., F. Inagaki, S. Nakagawa, H. Hirayama, T. Nunoura, Y. Sako, K. H. Nealson, and K. Horikoshi. 2003. Isolation and phylogenetic diversity of members of previously uncultivated epsilon-*Proteobacteria* in deep-sea hydrothermal fields. *FEMS Microbiol. Lett.* **218**:167–174.
50. Takai, K., A. Inoue, and K. Horikoshi. 2002. *Methanothermococcus okinawensis* sp. nov., a thermophilic, methane-producing archaeon isolated from a Western Pacific deep-sea hydrothermal vent system. *Int. J. Syst. Evol. Microbiol.* **52**:1089–1095.
51. Takai, K., T. Komatsu, F. Inagaki, and K. Horikoshi. 2001. Distribution of archaea in a black smoker chimney structure. *Appl. Environ. Microbiol.* **67**:3618–3629.
52. Takai, K., D. P. Moser, M. Deffau, T. C. Onstott, and J. K. Fredrickson. 2001. Archaeal diversity in waters from deep South African gold mines. *Appl. Environ. Microbiol.* **67**:5750–5760.
53. Tanner, M. A., B. M. Grobel, M. A. Dojka, and N. R. Pace. 1998. Specific ribosomal DNA sequences from diverse environmental settings correlate with experimental contaminants. *Appl. Environ. Microbiol.* **64**:3110–3113.
54. van der Maarel, M. J. E. C., R. R. E. Artz, R. Haanstra, and L. J. Forney. 1998. Association of marine archaea with the digestive tracts of two marine fish species. *Appl. Environ. Microbiol.* **64**:2894–2898.
55. Vetrani, C., A. L. Reysenbach, and J. Dore. 1998. Recovery and phylogenetic analysis of archaeal rRNA sequences from continental shelf sediments. *FEMS Microbiol. Lett.* **161**:83–88.
56. Vetrani, C., H. W. Jannasch, B. J. Macgregor, D. A. Stahl, and A. L. Reysenbach. 1999. Population structure and phylogenetic characterization of marine benthic archaea in deep-sea sediments. *Appl. Environ. Microbiol.* **65**:375–4384.
57. Von Damm, K. L. 1995. Controls on the chemistry and temporal variability of seafloor hydrothermal fluids, p. 222–247. *In* S. E. Humphris, R. A. Zierenberg, L. S. Mullineaux, and R. E. Tompson (ed.), *Geophysical monograph 91: seafloor hydrothermal system*. American Geophysical Union, Washington, D.C.
58. Wakeham, S. G., C. M. Lewis, E. C. Hopman, S. Schouten, and J. S. Sinninghe Damste. 2003. *Archaea* mediate anaerobic oxidation of methane in deep euxinic waters of the Black Sea. *Geochim. Cosmochim. Acta* **67**:1359–1374.
59. Wuchter, C., S. Schouten, H. T. S. Boschker, and J. S. Sinninghe Damste. 2003. Bicarbonate uptake by marine Crenarchaeota. *FEMS Microbiol. Lett.* **219**:203–207.